ASTRONOMY & ASTROPHYSICS
SUPPLEMENT SERIES

Astron. Astrophys. Suppl. Ser. **92,** 401-410 (1992)

The solar X-Ray/cosmic gamma-ray burst experiment aboard Ulysses

K. Hurley[1,4], M. Sommer[2], J.-L. Atteia[4], M. Boer[2], T. Cline[3], F. Cotin[4], J.-C. Henoux[6], S. Kane[1], P. Lowes[5], M. Niel[4], J. Van Rooijen[5] and G. Vedrenne[4]

[1] University of California, Space Sciences Laboratory, Berkeley, CA 94720, USA
[2] Max-Planck Institut für Extraterrestrische Physik, Giessenbachstrasse, 8046 Garching-bei München, Germany
[3] NASA–Goddard Space Flight Center, Code 661, Greenbelt, MD 20771, USA
[4] Centre d'Etude Spatiale des Rayonnements, B.P. 4346, 31029 Toulouse Cedex, France
[5] SRON–Laboratory for Space Research Utrecht, Sorbonnelaan 2, 3584 CA Utrecht, The Netherlands
[6] Observatoire de Meudon, DASOP, 5 Place Janssen, 92195 Meudon Principal Cedex, France

Received April 4; accepted August 19, 1991

Abstract. — We describe the scientific objectives of the Ulysses solar X-ray/cosmic gamma-ray burst experiment, and the unique features of the Ulysses mission which will help to achieve them. After a discussion of the special design constraints imposed by the mission, we describe the sensor systems, consisting of two CsI scintillators and two Si surface barrier detectors covering the energy range 5 keV–150 keV. Their operating modes and inflight performance are also given.

Key words: Gamma rays: Bursts, Sun: X-rays, Instruments.

1. Scientific objectives.

The Ulysses solar X-ray/cosmic gamma-ray burst instrument (acronym: GRB) has three main scientific objectives. The first is the study and monitoring of solar flare X-ray emission. The second is the detection and localization of cosmic gamma-ray bursts. The third is the *in-situ* detection of Jovian auroral X-radiation. We discuss each of these briefly in turn. For a review of experimental data on solar flare X-rays, see Dennis (1985, 1988). Reviews of cosmic gamma-ray burst observations have appeared in Hurley (1988, 1989).

Hard X-ray emission associated with solar flares was first detected in 1959 (Peterson and Winckler, 1959). It is caused by the bremsstrahlung of high energy, flare-produced electrons, on ions in the ambient solar atmosphere. The source of the energy for electron acceleration is generally agreed to be the solar magnetic field, and these electrons may account for half of the total flare energy. The site of X-ray production may vary from low altitudes to altitudes over 40,000 km. The spectral and temporal characteristics of solar flare hard X-rays are diverse, ranging from relatively soft, thermal ($kT \approx 40$ keV) spectra, to hard, power law spectra, and from microflares with durations of seconds (Lin *et al.*, 1981) to events lasting 30 minutes or more. Two examples are shown in Figures 1 and 2. Rapid fluctuations (tens of ms) in hard X-ray intensities have also been observed (Hurley *et al.*, 1983; Kiplinger *et al.*, 1983).

Stereoscopic observations of solar X-rays by spacecraft widely separated in heliocentric longitude have been carried out (see, e.g., Kane *et al.*, 1988, and references therein). They provide information on the altitude dependence of the X-ray emission, which in turn can be used to constrain electron acceleration models. (The altitude dependence follows from the observations when one or more spacecraft observes the event partially occulted by the solar limb.) These observations also allow a study of the directivity of the X-ray emission, which is related to the electron beaming (Vestrand *et al.*, 1987).

Cosmic gamma-ray bursts were discovered in 1973 by Klebesadel *et al.* They are typically 10-s long events with hard spectra extending to MeV energies. An example is shown in Figure 3. Their energy spectra display evidence of cyclotron features around 20 and 40 keV (Murakami *et al.*, 1988) and redshifted positron-electron annihilation radiation (Golenetskii *et al.*, 1986). These and other lines of evidence suggest that most gamma-ray bursts are associated with strongly magnetized galactic neutron stars. Nevertheless, the energy source of gamma-ray bursts is one of their outstanding mysteries. No unambiguous count-parts to gamma bursters have been identified in any wavelength

Send offprint requests to: K. Hurley.

range, despite deep searches in the radio, infrared, optical, and X-ray ranges. Thus it is not known whether the apparent neutron stars are single objects, or in binary systems. Consequently, it has proven impossible to choose between energy sources associated with lone neutron stars (e.g., starquakes) and sources associated with neutron stars having companions (e.g., accretion).

The only proven method for obtaining precise (arcminute and less) burster locations is arrival time analysis (or "triangulation") between widely separated spacecraft in an interplanetary network. Interspacecraft distances of several AU are required for good localization, since the characteristic dimension of an error box is inversely proportional to the spacecraft separation. Prior to the launch of Ulysses, interplanetary networks of burst detectors included missions to Venus (see, e.g., Atteia *et al.*, 1987) and Mars.

Jovian X-radiation was first detected by Metzger *et al.* (1983) using the Einstein satellite. X-rays in the 0.2-3 keV band were imaged with 4" resolution, and provided evidence that the sources of X-radiation were the Jovian north and south auroral zones. The origin of the X-rays could have been either electron bremsstrahlung in the Jovian upper atmosphere, or characteristic line emission from atmospheric atoms excited by heavy ions precipitating from the Io torus. These two models make very different predictions about the hard X-ray flux in the Ulysses GRB energy range.

2. Unique contribution of the Ulysses mission.

The Ulysses mission profile will contribute in a unique way to each of the objectives above. During the Jupiter-bound phase of the mission, the spacecraft explores a wide range of heliographic longitudes, making stereoscopic observations possible. It also monitors solar activity on portions of the solar disk invisible from Earth. In the out-of-ecliptic phase, and particularly during the polar passages, Ulysses will be situated at high solar latitudes, enabling it to view a large part of the Sun's equatorial regions where the majority of flares occur.

Ulysses is also the first spacecraft with a gamma-ray burst detector to travel beyond the orbit of Mars. This results in a triangulation baseline of unprecedented length. Consequently the localization accuracy for cosmic gamma-ray bursts will be the best ever achieved.

Finally, Ulysses will be the first mission to carry an X-ray detector to the Jovian magnetosphere, and thus the first to study Jovian X-radiation *in situ*.

3. GRB instrument design history and special requirements.

The GRB experiment was proposed in 1977 with a twin experiment aboard the NASA spacecraft. This approach had numerous advantages: a carefully intercalibrated pair of experiments at opposite ecliptic latitudes would survey the solar equatorial regions extensively, and stereoscopic observations would be relatively easy to compare with matched detectors. Triangulation baselines for cosmic gamma-ray bursts would be long, and the fact that two detectors in the network would be out of the ecliptic plane would provide a particularly favorable geometry for localization (non-coplanar detectors are required for arrival time analysis).

With the unique mission opportunities, however, came unique design constraints. A radiation-hardened microprocessor was required to survive the passage through the Jovian radiation belts; few were available during the design phase of the GRB experiment. The limited performance of the unit chosen dictated simplified operating modes for the experiment. Electrical power aboard Ulysses is provided by a radioisotope thermoelectric generator (RTG) containing 10 kg of ^{238}Pu (about 10^5 Ci). The GRB instrument would be the first cosmic gamma-ray burst detector to have to operate in this unfavorable background environment. To minimize the interference from the RTG, the sensors had to be mounted on the magnetometer boom, and were required to be essentially amagnetic. (More precisely, the remnant field could not exceed 2×10^{-5} G at 25 cm.) Finally, the mass and power allocations for the GRB experiment were small compared to inner planet missions–2 kg and 2.6 W, respectively.

4. The hard X-ray detectors.

The hard X-ray detector was designed to operate in the nominal energy range 15-150 keV. The design approach taken for this unit was to minimize the RTG-induced background

1) by minimizing the interaction cross section in the sensors for the high energy RTG gamma-rays,
2) by mounting the sensors as far as possible from the RTG,
3) by aligning them along the RTG axis to take advantage of the maximum self-absorption in the RTG itself, and
4) by mounting them so that the spacecraft provided passive shielding from the RTG.

Since a boom-mounted instrument far ($\approx$3 m) from the body of the spacecraft can have practically all-sky visibility, the sensor shape was chosen to have a nearly isotropic response. Criterion 1) above dictated the use of thin sensors. Thus hemispherical shell scintillators were chosen. CsI(Tl) was selected to minimize hermeticity problems.

The hard X-ray detection system is shown in Figure 4. It consists of two 3-mm thick by 51-mm diameter CsI(Tl) crystals mounted via a plastic light guide to two photomultiplier tubes. Initially, the photomultiplier tubes were RCA developmental units (C70132D) with convex photocathodes, which minimized the light guide volume. However, in the long waiting period between fabrication and launch, the tubes became noisy, apparently due to absorption of air at the glass-to-metal interfaces. In 1987, it was decided to retrofit new sensor units to the experiment, and as the RCA tube was no longer available, the Hamamatsu R1924 was selected. It is a ten-stage ruggedized tube with a one-inch diameter photocathode; its mass is about 19 g. Tubes with both borosilicate glass and quartz windows were tested, since a potential radiation damage problem was anticipated during the Jupiter flyby. Following a re-evaluation of the radiation damage problem, the borosilicate tubes (which had superior performance) were judged acceptable, and were selected for the flight model. CsI(Tl) cylinders were supplied by Bicron Corporation. Crystal machining, packaging, and mounting to the phototubes was done by MBB. Dornier Systems had overall responsibility for the design and fabrication of the detector assembly, including the analog electronics, under the direction of the Max-Planck Institute.

5. The soft X-ray detectors.

The soft X-ray sensors were designed as solar X-ray monitors for the energy range ≈5-20 keV. They consist of two 500-μm-thick, 0.5-cm^2-area Si surface barrier detectors manufactured by the Ortec Corporation. A 100 mg/cm^2 beryllium foil front window rejects low energy X-rays and defines a conical field of view of 75° half-angle. Detectors and front-end electronics are mounted in a cubic housing covered on four sides with an optical solar reflective coating for passive cooling. The detectors operate in the temperature range -35°C to -55°C. The amplified pulses of the two Si detectors are analyzed by a hybrid stack of six-level discriminators which define four differential energy channels and two integral channels. The soft X-ray detector system is shown in Figure 5; it was built by the SRON Laboratory for Space Research at Utrecht.

6. Digital electronics.

The digital electronics package is mounted on the spacecraft platform, and contains the data processing electronics for both sensor systems. It provides:

1) six accumulators for the soft X-ray instrument,
2) four real-time accumulators, two trigger circuits, and a 32 kbit memory managed by an 1802 microprocessor to store background spectra and count rates, calibration spectra, and pretrigger and event data, all for the hard X-ray instrument,
3) one counter for timing,
4) state-of-health monitoring, and
5) command processing.

Count rates from the six channels of one or both of the two Si detectors are accumulated in 19-to-8 bit accumulator/compressors. These data are multiplexed and incorporated into the data stream through one of the five 8-bit telemetry words allocated to the GRB instrument in each spacecraft telemetry frame. Data from the hard X-ray experiment are read out through the remaining four words.

Approximately 50 parameters related to the state of health and mode of operation of the instrument are monitored through three analog lines and one multiplexed 8-bit housekeeping data word. Programs for the microprocessor are stored in two redundant ROMs, selectable by command. When the experiment is turned on, nominal parameters included in the programs are stored in a small RAM. It is therefore possible to modify these parameters through a direct memory access.

The digital electronics were the responsibility of the Centre d'Etude Spatiale des Rayonnements, and were fabricated by Crouzet S.A. A more complete description of this system, including a block diagram, has been published (Cotin *et al.*, 1983).

7. Operating modes.

The Ulysses spacecraft can operate at one of four data rates: 1024, 512, 256, or 128 b/s. The time resolution of some GRB modes varies with the spacecraft data rate. In the following description, these time resolutions are given for the highest data rate, and scale directly in proportion to the actual spacecraft data rate. The telemetry allocation for the GRB instrument is 40 b/s when the spacecraft data rate is 1024 b/s.

Table 1 summarizes the operation of the soft X-ray detectors, which measure X-radiation in the energy range above ~ 5 keV in six channels. Either one or both of the two Si detector count rates can be read out.

The hard X-ray instrument changes its operating modes depending upon 1) the count rates which it measures, 2) the ground commands which it receives, and 3) the changes in the spacecraft telemetry mode. In the absence of a burst, the instrument operates in one of two waiting modes (operation mode 1 or 2, selectable by command). When a burst is detected, a trigger signal is issued and the instrument switches into a burst mode to record high time resolution data in memory; these data are read out slowly into the telemetry stream. The entry into burst mode may also be selected by command. At the end of the burst readout cycle, the experiment switches automatically into a calibration mode. In addition, the calibration

mode is automatically selected when the spacecraft goes from 512 b/s to 1024 b/s (approximately once/day); it may also be selected by command. The various modes of the instrument will now be described in more detail. Note that some solar and cosmic events which do not trigger the experiment can still be detected in the real-time data of the waiting modes.

In Operation Mode 1, the outputs of the two hard X-ray detectors are summed, and integral count rates are transmitted with 0.25-s time resolution in the 1024 b/s mode. In Operation Mode 2, the outputs of the two detectors are also summed, but the integral count rates are transmitted with 0.5-s time resolution in the 1024 b/s mode. In addition, in this mode, four-channel energy spectra are transmitted from each detector. The four energy channels are determined by summing channels from the output of a 64-channel pulse height analyzer, and are identical for the two detectors. The time resolution of the energy spectra is 8 s in the 1024 b/s mode.

The instrument may go into the burst mode by command, or automatically when the count rate exceeds a certain threshold. In this mode high time resolution count rates and energy spectra are recorded for a short period of time, corresponding to a solar flare or a cosmic gamma-ray burst. In order to determine whether an automatic trigger should be issued, the instrument compares the integral count rates with backgrounds in two energy ranges simultaneously; the energy levels are defined by lower, medium, and upper level discriminators (adjustable by command). The range of adjustment starts around 15 keV and ends around 150 keV. Each of the two comparisons takes place over a time interval which may be selected from four possible values; these two intervals may be different for the two energy levels. The lower level trigger time intervals are 0.125, 0.25, 0.5, and 1 s; the upper level times are 0.5, 1, 2, and 4 s. Each trigger time interval has an associated burst threshold, set by command, in counts; thus the thresholds do not vary according to the background counting rates.

Following a burst trigger, high time resolution data are written into the experiment memories; then the data are read out. During write mode, the data which appear in the telemetry stream consist of integral count rates with 0.5-s resolution in the 1024 b/s mode. The burst data, read out later, consist of:

1) Either 16 s of 8-ms integral count rates, or 64 s of 32-ms integral count rates (selectable by command), from the sum of the two detectors, and
2) 16-channel energy spectra from the sum of the two detectors; either
   a) 16 1-s spectra, 16 2-s spectra, and 28 16-s spectra (a total of 496 s), or
   b) 16 2-s spectra, 16 4-s spectra, and 28 32-s spectra (a total of 992 s).

The choice between the two is made by command. Data readout requires approximately 35 minutes at 1024 b/s; during this time the experiment does not accept a second trigger signal, although burst data can still be acquired in the real-time mode.

The calibration mode is used to calibrate the gains of the two detectors. A weak ^{241}Am source provides a 60-keV peak which can be detected in the energy spectra. The calibration mode data consist of 32 spectra, integrated over 64 s, for each detector. As the data are read out, 0.5-s resolution count rate data from the sum of the two detectors are also output to the telemetry, so the experiment can detect bursts in real time. In addition, an increase in the count rate can trigger the burst detection circuit and override the calibration mode.

8. In-flight performance and initial results.

The experiment was turned on November 9, 1990, and has been in almost continuous operation since then. The hard X-ray instrument has detected an average of 2-3 solar flare X-ray events per day (see Fig. 1 and 2), and numerous other events, some of which are probably cosmic gamma-ray bursts, but which have not yet been confirmed by other spacecraft. (A confirmed event is shown in Fig. 3). A background spectrum, taken in the calibration mode, is shown in Figure 6. The background is comparable to that of other experiments operating in interplanetary space. The trigger levels are currently set at count rates corresponding to slightly less than 8σ above the background. Based on a cosmic gamma-ray burst which was observed by both the WATCH experiment aboard the GRANAT spacecraft (Lund, 1991) and Ulysses on February 19, 1991, we estimate the trigger sensitivity to be about 10^{-6} erg/cm^2, or in flux units, 10^{-7} erg/cm^2 s. Observations of a particularly intense solar flare on March 4, 1991 have confirmed that the hard X-ray detector suffers negligible dead time losses at count rates up to about 2×10^5 counts/s.

A key aspect of the Ulysses GRB scientific objectives is the comparison of Ulysses data with X-ray data taken on other spacecraft, as well as with optical data from ground-based all-sky monitors searching for optical flashes coincident with gamma-ray bursts. Figure 7 shows the experiments which are expected to be in operation over the nominal Ulysses lifetime. The presence of numerous gamma-ray burst and solar X-ray instruments in near-Earth orbit and interplanetary space promises to enhance the scientific return from Ulysses and advance our understanding of these two phenomena.

Acknowledgements.

Work on the digital electronics was supported at the CESR in France by the Centre National d'Etudes Spatiales. At the Max-Planck Institute this effort was sup-

ported by FRG Contracts 01 ON 088 ZA/WRK 275/4-7.12 and 01 ON 88014. K.H. gratefully acknowledges assistance from JPL Contract 958056.

References

Atteia J.-L., Barat C., Hurley K., Niel M., Vedrenne G., Evans W., Fenimore E., Klebesadel R., Laros J., Cline T., Desai U., Teegarden B., Estulin I., Zenchenko V., Kuznetsov A., Kurt V. 1987, ApJS 64, 305

Cotin F., deJager C., Henoux J.-C., Heise J., Hilhorst M., Hurley K., Niel M., Paschmann G., Sommer M., Van Rooijen J., Vedrenne G. 1983, in The International Solar Polar Mission–Its Scientific Investigations, ESA SP-1050, K.-P. Wenzel, R.G. Marsden, and B. Battrick Eds., (European Space Agency), p. 211

Dennis B. 1985, Solar Phys. 100, 465

Dennis B. 1988, Solar Phys. 1180, 49

Golenetskii S., Mazets E., Aptekar R., Guryan Yu., Ilyinskii V. 1986, Ap&SS 124, 243

Hurley K. 1988, in Cosmic Gamma Rays, Neutrinos, and Related Astrophysics, NATO ASI Series C 270,M. Shapiro and J. Wefel Eds., (Kluwer Academic Publishers - Dordrecht), p. 337

Hurley K. 1989, in Fourteenth Texas Symposium on Relativistic Astrophysics, Ann. N.Y. Acad. Sci. 571, E.J. Fenyves Ed., p. 442

Hurley K., Niel M., Talon R., Estulin I., Dolidze V. 1983, ApJ 265, 1076

Kane S., Fenimore E., Klebesadel R., Laros J. 1988, ApJ 326, 1017

Kiplinger A., Dennis B., Emslie A., Frost K., Orwig L. 1983, ApJ 265, L99

Klebesadel R., Strong I., Olson R. 1973, ApJ 182, L85

Lin R., Schwartz R., Pelling R., Hurley K. 1981, ApJ 251, L109

Lund N. 1991, IAU Circular 5193, February 21

Metzger A., Gilman D., Luthey J., Hurley K., Schnopper H., Seward F., Sullivan J. 1983, J. Geophys. Res. 88, 7731

Murakami T., Fujii M., Hayashida K., Itoh M., Nishimura J., Yamagami T., Conner J., Evans W., Fenimore E., Klebesadel R., Yoshida A., Kondo I., Kawai N. 1988, Nature 335, 234

Peterson L., Winckler J. 1959, J. Geophys. Res. 64, 697

Vestrand W., Forrest D., Chupp E., Rieger E., Share G. 1987, ApJ 322, 1010

TABLE 1. *Soft X-Ray Data.*

Energy Range, keV	>3.5[a]	5-7.1	7.1-10	10-14	14-20	>20
Time Resolution (s)[b]	8	4	4	4	16	16
Counter Capacity	507904	507904	507904	507904	507904	507904

[a] Noise channel, used to help calibrate the instrument
[b] At 1024 b/s telemetry rate; scales directly with other TM rates

TABLE 2. *Summary of GRB Experiment Operating Modes*

Detector	Parameter Analyzed	Time Resolution (secs)	Storage Time (secs)	Data Compression	Counter/ Memory Capacity	Comments
Operation Mode 1						
HUS 2A	Count Rates	0.25[a]	N/A	n(n+1)/2	32640	Σ2 Detectors
Operation Mode 2						
HUS 2A	Count Rates	0.5[a]	N/A	n(n+1)/2	32640	Σ2 Detectors
HUS 2A	Energy Spectra	8[a]	N/A	none	65535	
Burst Data Write Mode						
HUS 2A	Count Rates	0.5[a]	N/A	n(n+1)/2	32640	Σ2 Detectors
Burst Data Readout Mode						
HUS 2A	Count Rates	0.5[a]	N/A	n(n+1)/2	32640	Σ2 Detectors
HUS 2A	Count Rates	0.008	16	none	255	Σ2 Detectors
HUS 2A	Count Rates	0.032	64	÷1, 2, 4, or 8	959	Σ2 Detectors
HUS 2A	Energy Spectra	1-32	496-992	none	65535	Σ2 Detectors
Calibration Mode						
HUS 2A	Count Rates	0.5[a]	N/A	n(n+1)/2	32640	Σ2 Detectors
HUS 2A	Energy Spectra	32	N/A	none	65535	

[a] Time resolution for 1024 b/s; scales with spacecraft telemetry rate

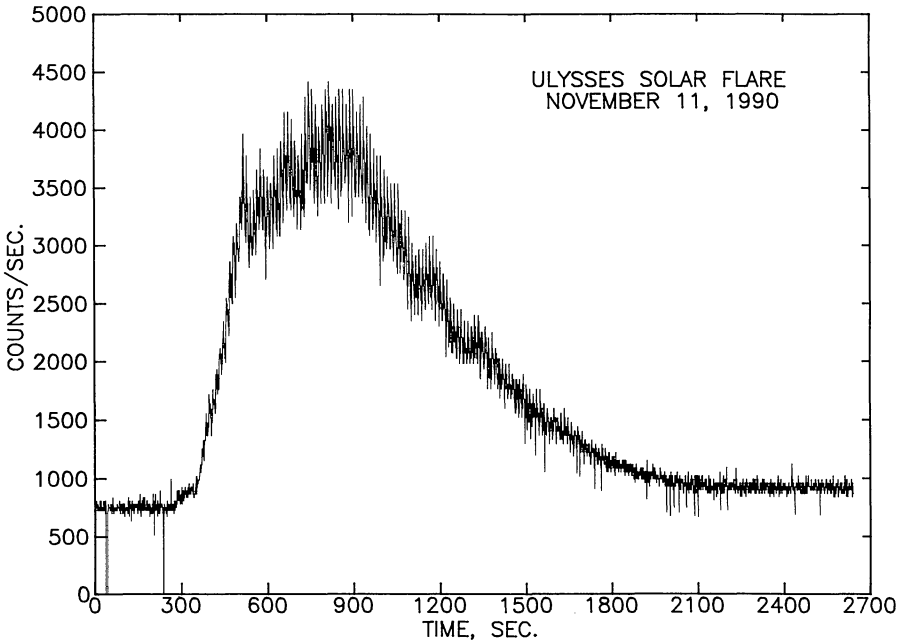

FIGURE 1. Solar flare X-rays observed by the GRB detector on November 11, 1990. The peak occurs around 04:30 UT. Due to the fact that the detector axis points towards the Earth, and the Earth-Ulysses-Sun angle was large, 10-s spin modulation can be observed in the time history.

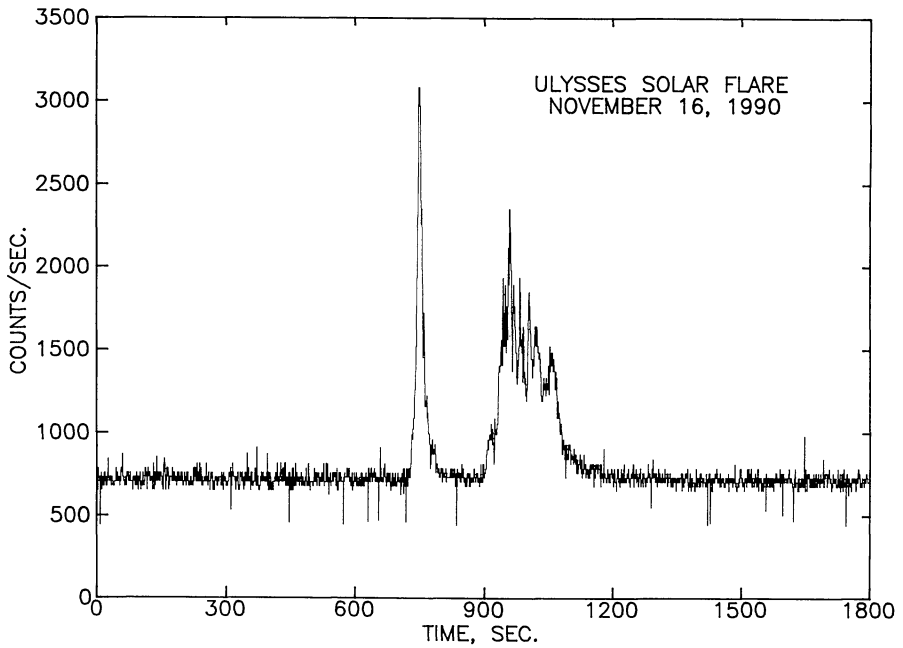

FIGURE 2. Solar flare X-rays observed by the GRB detector on November 16, 1990. The first peak is around 13:12 UT. Spin modulation can be observed on the second peak.

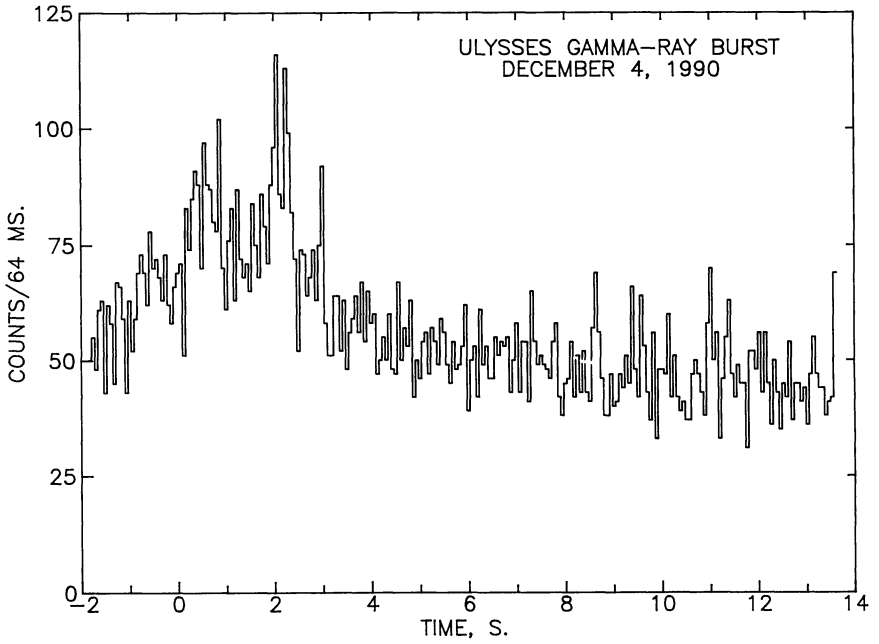

FIGURE 3. A cosmic gamma ray burst detected by Ulysses on December 4, 1990 around 9:30 UT. The time history in the 20-150 keV range is shown with 64-ms resolution. This event was also detected by Pioneer Venus Orbiter (R. Klebesadel, private communication).

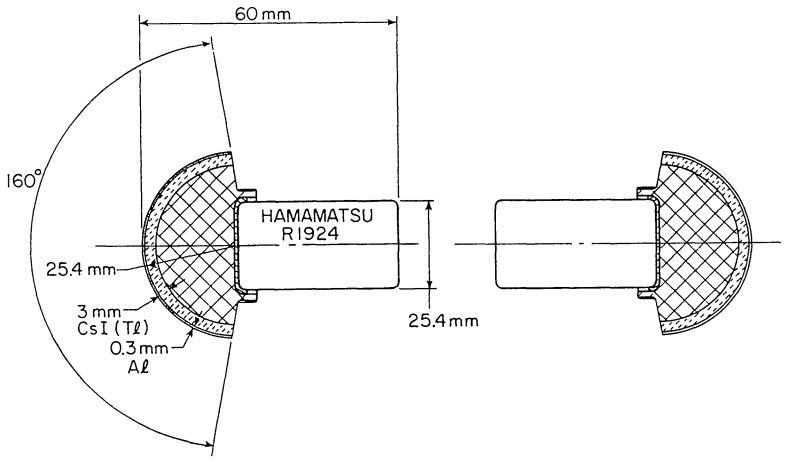

FIGURE 4. The hard X-ray detectors. The axis points towards Earth. Each unit contains a 10-nCi ^{241}Am source for inflight calibration. The energy resolution is about 40% at 60 keV, and the noise threshold around 10 keV, in the laboratory at ambient temperature.

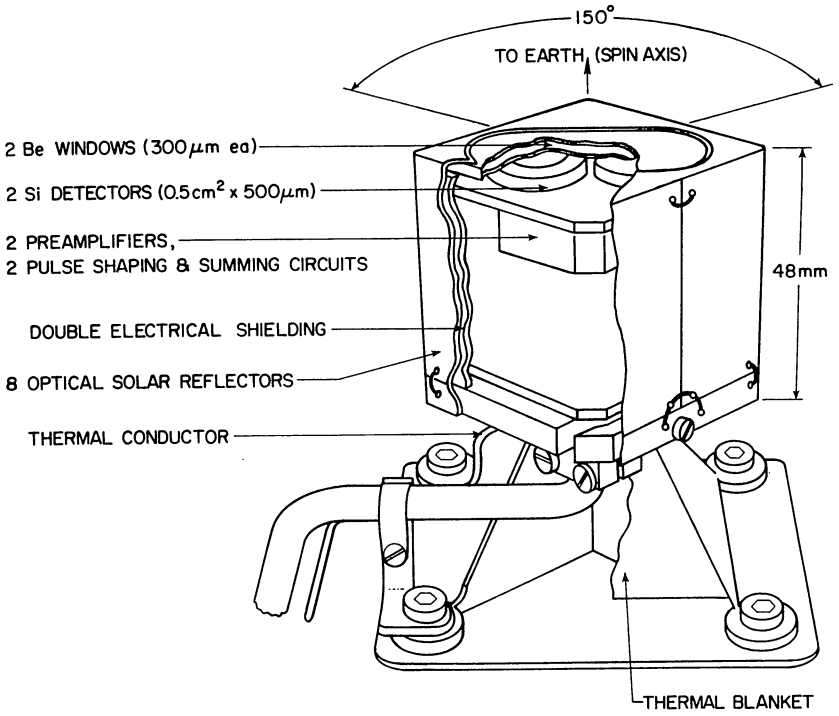

FIGURE 5. The soft X-ray detectors. The two Si surface barrier detectors point towards the Earth. Inflight calibration is provided by two 20-nCi ^{129}I sources.

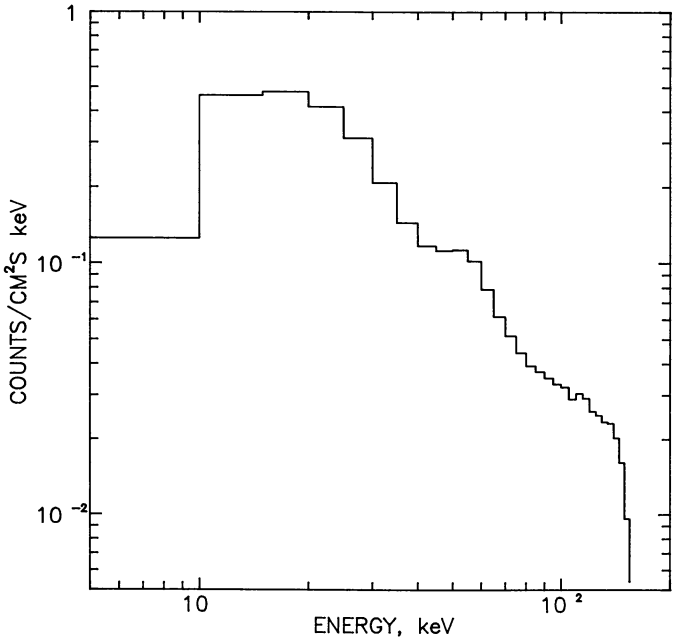

FIGURE 6. Background spectrum from one of the hard X-ray detectors, taken in the calibration mode. The 60-keV ^{241}Am peak is visible.

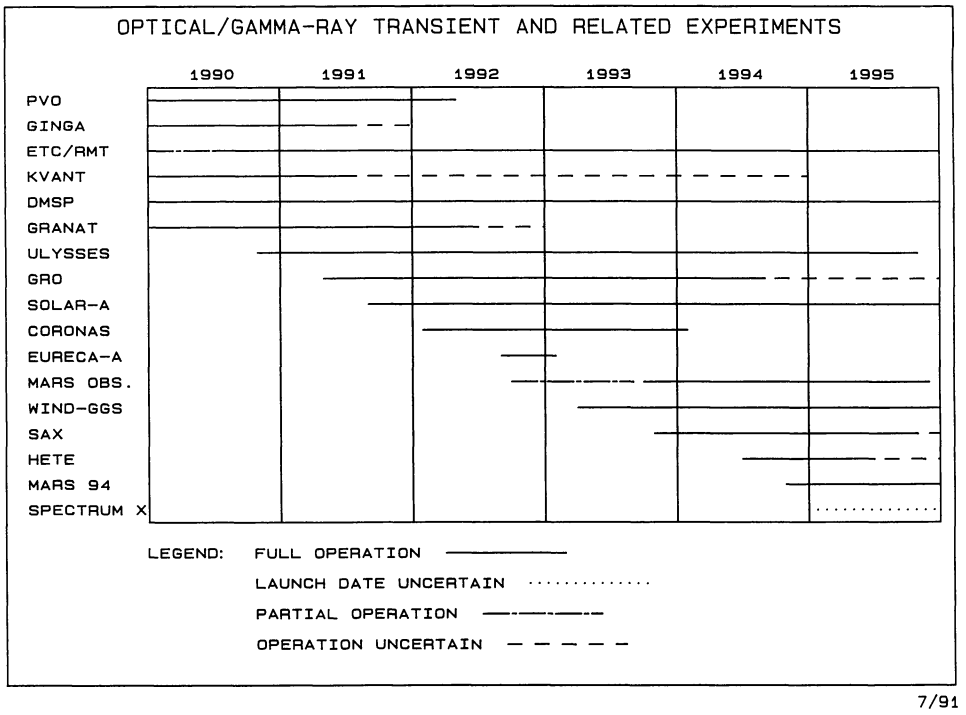

FIGURE 7. Experiments operating in conjunction with Ulysses. PVO: Pioneer Venus Orbiter; Ginga: Japanese near-Earth spacecraft; ETC/RMT: Explosive Transient Camera/Rapidly Moving Telescope, a ground-based all-sky monitoring system at Kitt Peak; Kvant: module aboard the Soviet MIR space station; DMSP: Defense Meteorological Satellite Program; GRANAT: Franco-Soviet gamma-ray satellite; GRO: NASA's Gamma Ray Observatory; Solar-A: Japanese satellite for solar studies; CORONAS: Soviet satellites for solar studies; EURECA-A: WATCH gamma-ray burst experiment; Mars Obs.: NASA's Mars Observer, with a Ge experiment modified to detect gamma-ray bursts; Wind-GGS: part of NASA's Global Geospace Science program, with a Ge detector for gamma-ray bursts; SAX: Italian X-ray astronomy satellite; HETE: NASA's High Energy Transient Experiment; Mars 94: Soviet Mars mission, with gamma-ray burst experiments; Spectrum X: Soviet X-ray satellite.